A Collection of Airborne Measurements and Analyses of Trace Gases Emitted from Multiple Fires in California

Laura T. Iraci[1], Caroline L. Parworth[1,†], Emma L. Yates[1,2], Josette E. Marrero[1,‡], Ju-Mee Ryoo[1,3]

[1]NASA Ames Research Center, Moffett Field, CA, USA. [2]Bay Area Environmental Research Institute, Moffett Field, CA, USA. [3]Science and Technology Corporation, Moffett Field, CA, USA.

Corresponding author: Laura T. Iraci (Laura.T.Iraci@NASA.gov)

†Now at Aclima, Inc., San Francisco, CA, USA

‡Now at Sonoma Technology Inc.

Key Points:

- Trace gas observations near/around 12 wildfires and 1 prescribed fire (2013 – 17) highlight variability of many fires over multiple years
- 5 flights to Soberanes fire, providing trace gas and wind measurements over the lifetime of the megafire
- Several downwind legs and regional transits also included, making possible contributions to studies of human exposure at regional scales

Abstract

Biomass burning is an important source of trace gases and particles, and can influence air quality on local, regional, and global scales. With the threat of wildfire events increasing due to changes in land use, increasing population, and climate change, the importance of characterizing wildfire emissions is vital. In this work we characterize trace gas emissions from 12 wildfires and 1 prescribed fire in California between 2013 and 2017, in some cases with multiple measurements performed during different burn periods of a specific fire. Airborne measurements of carbon dioxide, methane, ozone, formaldehyde, water vapor, temperature and 3-dimensional winds were made by the Alpha Jet Atmospheric eXperiment (AJAX) and [has been/will soon be] published at NASA's Airborne Science Data Center (doi:10.5067/ASDC/AJAX/wildfire). The majority of these measurements were made as close as possible to each fire and represent fresh emissions from known fire sources. This set of observations from 13 different fires offers the opportunity to explore trace gas emissions over a range of meteorology, fire conditions, and to a lesser extent, vegetation type and drought, and adds to the body of knowledge collected by other investigators and field campaigns.

Plain Language Summary

Biomass burning is an important source of trace gases and particles which can influence air quality on local, regional, and global scales. This set of airborne observations of trace pollutants and winds from 13 different fires broadens the range of fire types and conditions for which observations have been made near the top of visible smoke plumes. Calibrated and quality-controlled observations of methane, formaldehyde, ozone, carbon dioxide, water vapor and 3-D winds near to a variety of active fires offer the opportunity to explore emissions over a range of meteorology, fire conditions, and to a lesser extent, vegetation type and drought. This dataset can also be an asset for bridging the gap of knowledge between models and in situ data collected by other investigators and field campaigns.

1 Introduction

Wildfires in California can influence local, regional, and global air quality (Jaffe et al., 2020, Gupta et al. 2018, McClure & Jaffe, 2018; Singh et al., 2010; Yates et al., 2016), and the duration and frequency of wildfires is increasing associated with increased human population and climate change (Holden et al., 2018; Radeloff et al., 2018; Westerling et al., 2006). The trend toward increasing area burned in recent decades is influenced by multiple factors that vary regionally, and thus relevant data is needed at a variety of spatial scales (Jaffe et al., 2020). With more than a quarter of California residents living under "very high" or "extreme" fire threat (CARB, 2021) and an increasing awareness of the toxicity of wildfire smoke (e.g., Aguilera et al., 2021), it is important to understand the range of conditions, emissions, and impacts from the variety of small and large fires that occur in California each year.

Fixed-location surface sites offer multi-year archives of site-specific observations of aged, advected smoke (Buysse et al., 2019), and large field campaigns such as the recent Fire Influence on Regional to Global Environments and Air Quality (FIREX-AQ) and Western wildfire Experiment for Cloud chemistry, Aerosol absorption and Nitrogen (WE-CAN) missions can bring together multi-disciplinary teams with skills and tools applied across the fuel-fire-smoke system for an intensive measurement period.

We report here a different type of field campaign occurring over multiple years, sampling trace gases emitted by fires with a range of size, intensity, and meteorological conditions. In this way, the data set reported here is complementary to both other paradigms. By sampling near to the source, the AJAX project adds the perspective of fresh emissions for a variety of fires over both very active burning years and those which are less so. Measurements of fresh fire emissions are particularly needed because they represent the starting point in current global atmospheric chemistry models and smaller-scale photochemical plume models (Akagi et al., 2011). In particular, Liu et al. (2019) demonstrate the need for near-fire measurements of ozone, CO_2, VOCs and winds.

In this work we report observations of trace gases (ozone (O_3), carbon dioxide (CO_2), methane, (CH_4) and formaldehyde (HCHO)) and in situ temperature and winds, as well as derived analyses used to characterize emissions from 12 wildfires and 1 prescribed fire in California between 2013 and 2017, broadening the knowledge base of fire emissions available to the community. One example is presented in detail, and the application of the data to calculation of Emission Ratios (ERs) is presented.

2 Data Set

2.1 Airborne Trace Gas and Meteorological Measurements

The Alpha Jet Atmospheric eXperiment (AJAX) has been making in situ airborne measurements of trace gases on a regular, long-term basis, with 229 flights between 2011 and 2018. AJAX measures O_3, CO_2, CH_4, HCHO, water (H_2O), and meteorological parameters (ambient pressure, temperature, and 3-D winds). A detailed description of AJAX and instrument placement can be found in Hamill et al. (2016). Measurements of CO_2 and CH_4 are taken with a cavity ring-down spectrometer (CRDS, Picarro G2301-m) (Tadić et al., 2014; Tanaka et al., 2016). Measurements of O_3 use a modified UV monitor (2B Technologies, Inc., model 205) (Yates et al., 2013). Airborne measurements of HCHO are taken with the Compact Formaldehyde Fluorescence Experiment (COFFEE) (St. Clair et al., 2017) beginning in December 2015.

Figure 1 shows the location for each fire sampled by AJAX. Flights typically occurred during the early afternoon (12 – 2 PM local time), and most data were collected at altitudes near the top of the visible smoke plume. During analysis, fire plumes were identified by choosing sections of each flight when mixing ratios of trace gases were well above their background values, and when winds were coming from the general direction of the fire.

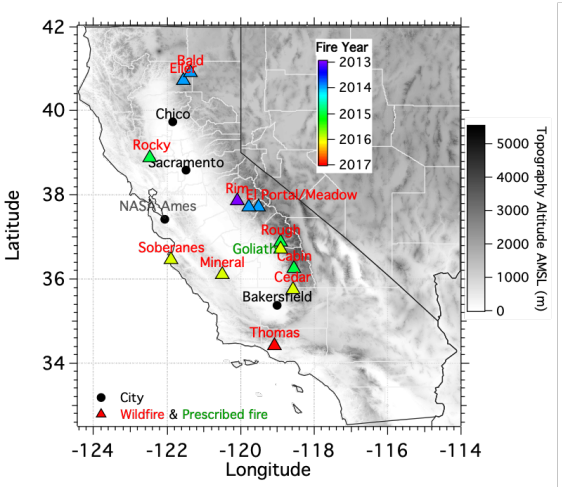

Figure 1. A topographic map with the location of fires measured by AJAX, colored by year.

The in situ trace gas measurements have been calibrated, screened for quality, and archived as comma separated variable (CSV) files in ICARTT format with a common time index. Ozone data have been post-processed with the results of an eight-point calibration (ranging from 0 to 300 ppbv) performed before and after each flight using a NIST-traceable

calibration source (2B Technologies, model 306) referenced to the WMO scale. Calibration settings for the O_3 monitor were left at manufacturer default settings during flight, and corrections to account for linearity offset and zero offset have been applied during data processing and are documented in each data file. Data have been averaged to 10 seconds and the inlet delay (lag time) has been subtracted; uncertainty estimates are included and are generally on the order of 3 ppbv. Quality assurance methods focus primarily on instrument pump performance; instrument temperature is a secondary diagnostic which has been evaluated. Data have been discarded if either characteristic is out of specification.

Ozone measurements were obtained with a commercial UV monitor with hopcalite scrubber and Nafion dryer. This technique has been shown to be free of interferences in aged wildfire plumes with ≤800 ppb CO (Gao & Jaffe, 2017). It is also the method found by Long et al. (2021) to have a relatively small interference (i.e., 1.5 – 3 ppb O_3 (ppm CO)$^{-1}$) compared to our calibration uncertainly (± 3 ppbv), indicating that a statistically robust interference would be present only in situations when sampling well in excess of 1000 ppb CO. Unfortunately CO measurements are not available in the AJAX payload, but the visibility, airspace, and safety limitations of the AJAX flight plans require operations outside the dense plume. Comparison with data collected by the chemiluminescence technique during the SEAC4RS campaign indicate that AJAX ozone measurements were not subject to significant interferences at least up to ΔCO_2 ~40 ppm and ΔCH_4 ~300 ppb (Yates et al., 2016).

CO_2 and CH_4 data have been post-processed to traceable standard scales by comparison to standards prepared by the Global Monitoring Division of the National Oceanic and Atmospheric Administration (NOAA). CO_2 is given on the WMO mole fraction scale version X2007, and CH_4 is tied to the NOAA04 and X2004A scales, with calibration factors and additional details given in the individual data files. Water vapor corrections determined by Chen et al. (2010) have been applied to calculate the dry mixing ratios of CO_2 and CH_4, and uncertainty estimates based on propagation of errors are documented. The most important quality assurance step for this data product evaluates instrument optical cavity pressure and temperature for nominal conditions. The inlet lag time has been accounted for, and data have been averaged to 3 seconds.

Meteorological data (temperature, pressure and 3-dimensional winds) and formaldehyde observations are provided at 1 Hz in ICARTT-compliant text files. The root mean square accuracy of the pressure and temperature measurements from the Meteorological Measurement System (MMS) are ±0.3 hPa and ± 0.3 K, respectively. The 1-σ uncertainty of the 3-D wind vector is ± 1.0 m/s. The overall measurement uncertainty for HCHO is estimated to be 20% of [HCHO] + 100 pptv (St. Clair et al., 2017).

2.2 Additional Observations and Analyses

For each flight, the age of each fire plume sampled was approximated by dividing the horizontal sampling distance from the fire source by the average wind speed at the altitude where the smoke was sampled. For the 3 flights when in situ wind speed and direction measurements were unavailable, average wind speeds were derived from hourly ERA5 reanalysis data (Hersbach et al., 2020). Specific findings from individual flights are presented in Tables 1-3.

Parameters related to the fire properties were collected from multiple sources. Fire Radiative Power (FRP) data was obtained from NASA's Visible Imaging Radiometer Suite

(VIIRS) 375 m fire data aboard the National Polar-orbiting Partnership (S-NPP) satellite (Earthdata, 2019). Burn scar areas for wildfires were obtained from the Geospatial Multi-Agency Coordination (GeoMAC) database (Walters et al., 2011). Land cover data was obtained from the US Geological Survey National Land Cover Database (NLCD). The type of vegetation burned in each fire of this study was obtained from the Fuel Characteristic Classification System (FCCS) developed by the US Forest Service (Ottmar et al., 2007; Riccardi et al., 2007).

Meteorological conditions from nearby California Resource Board (CARB) ground sites were obtained from the CARB Air Quality and Meteorological Information System (AQMIS) website, compiled and analyzed, and are included in Tables 1-3.

To illustrate the transport pathways and potential sources of airmasses measured along each flight, back trajectories were computed using the Hybrid Single-Particle Lagrangian Integrated Trajectory (HYSPLIT) model (Stein et al., 2015). 72-hour back trajectories were computed every one hour during the same time period as each AJAX fire flight based on the large-scale meteorological fields available from the National Oceanic and Atmospheric Administration (NOAA) Global Data Assimilation System (GDAS, 1° grid spacing). All of the back trajectories originated from the aircraft altitude along each point of the flight, and vertical transport was based on the mean vertical velocities from GDAS. These analyses were particularly useful for identifying segments of flights tracks which were influenced by nearby urban areas (e.g., Visalia and Bakersfield during portions of Flight 168) and for tracing the aged plume sampled from the Thomas fire (Flight 216).

NOAA's Hazard Mapping System Fire and Smoke product was also used to verify the assignment of smoke origin on several flight days, particularly when a sampled plume was likely generated by more than one fire (e.g., Rough and Cabin fires in 2015, Flight 167).

Collection of these relevant parameters and analyses into a single repository, along with the trace gas measurements, reduces the effort required in future studies of the variability among emissions from different fires.

2.3 Example of Available Data for Individual Flights

Each flight in the archive was analyzed in detail, and one example is shown in Figure 2. The Soberanes fire burned a total of 103,242 acres of Redwood and Tanoak forest from July 22 through October 12, 2016, allowing the AJAX project to sample emissions from this fire on five separate flight days.

As shown in Figure 2(k), Flight 197 on August 9 included several loops around the perimeter of the fire at a mean altitude of 2013 m, followed by a 91 km leg downwind of the fire at a mean altitude of 2129 m. The portions of the flight track edged in black correspond to the periods of time highlighted in gray in panels (a-f). Structured enhancements in CO_2, CH_4, O_3, HCHO, and H_2O are all evident when sampling to the east of the fire, consistent with both wind direction measured onboard and HYSPLIT analyses (not shown here but available in the archive).

When sampling around the perimeter of the fire, the intercepted plume was estimated to be ~2 hr old (relatively fresh). When sampling downwind (pale blue edging in Figure 2(k) and pale blue bars in panels (a-f)), the smoke was estimated to be ~8.5 hours old, and the trace gas mixing ratios are considerably smaller and less structured. Background mixing ratios were determined during a section of flight upwind of the fire (cyan highlighting in panels (a-f)), and

195 maximum enhancements in the fresh fire plume relative to this background were observed to be
196 ΔCH_4 = 619.1 ppb, ΔCO_2 = 37.9 ppm, ΔO_3 = 64.6 ppb, and ΔHCHO = 60.2 ppb (right hand axes
197 in panels (b-e)). In the aged portion ΔCH_4 = 38.4 ppb, ΔCO_2 = 3.5 ppm, and ΔHCHO = 4.3 ppb
198 were observed.

199

200 **Table 1.** Information on each California fire measured by AJAX in 2013 and 2014. Units are in
201 square brackets. "N/A" indicates data which are not available due to instrument failure.
202

Fire	Rim		El Portal	Bald	Eiler	Meadow
Vegetation Types	Live oak Blue oak woodland		Jeffrey pine, Red fir, White fir / Greenleaf manzanita Snowbrush forest	Scrub oak Chaparral shrubland	Red fir forest	Red fir forest
Total Acres Burned	257,314		4689	39,736	32,416	4772
Duration of Fire	8/17/13–10/27/13		7/26/14–8/4/14	7/30/14–8/16/14	7/31/14 – 8/24/14	8/15/14–9/29/14
Flight Date (Flight #)	8/29/13 (100)	9/10/13 (101)	7/29/14 (136)	8/6/14 (137)		9/9/14 (141)
Avg. RH at Ground Site [%]	59	39	39	100		46
Max. Temperature at Ground Site [°C]	26	24	27	23		22
Resultant Wind Speed at Ground Site (m/s)	12.1	10.1	7.8	2.2		8.2
Avg. Fire Radiative Power (±1σ) (FRP) [MW]	61.2 (±73.0)	14.2 (±11.0)	13.5 (±6.3)	N/A		21.1 (±8.8)
Avg. GPS altitude in fire plume (±1σ) [km]	4.4 (±0.004)	3.8 (±0.1)	2.7 (±0.4)	1.7 (±0.3)		3.9 (±0.1)
Age of fire plume [hr]	0.9	4.4	0.25	8.3		1.6
Avg. Distance from Fire Source (±1σ) [km]	45.4 (±2.8)	37.0 (±10.9)	13.2 (±6.5)	49.9 (±19.1)		12.4 (±5.5)
Average H_2O in plume (±1σ) [%v]	0.26 (±0.11)	0.68 (±0.19)	1.05 (±0.05)	1.29 (±0.19)		0.13 (±0.11)
Max ΔCH_4 in plume [ppb]	312.0	159.0	145.0	89.3		68.8
Max ΔCO_2 in plume [ppm]	41.1	9.91	16.3	23.5		7.1
Max ΔO_3 in plume [ppb]	105	N/A	18.5	N/A		-
ER_{CH4}	6.7	18.3	11.3	4.0		9.53
ER_{O3}	2.0	N/A	2.0	N/A		-

203

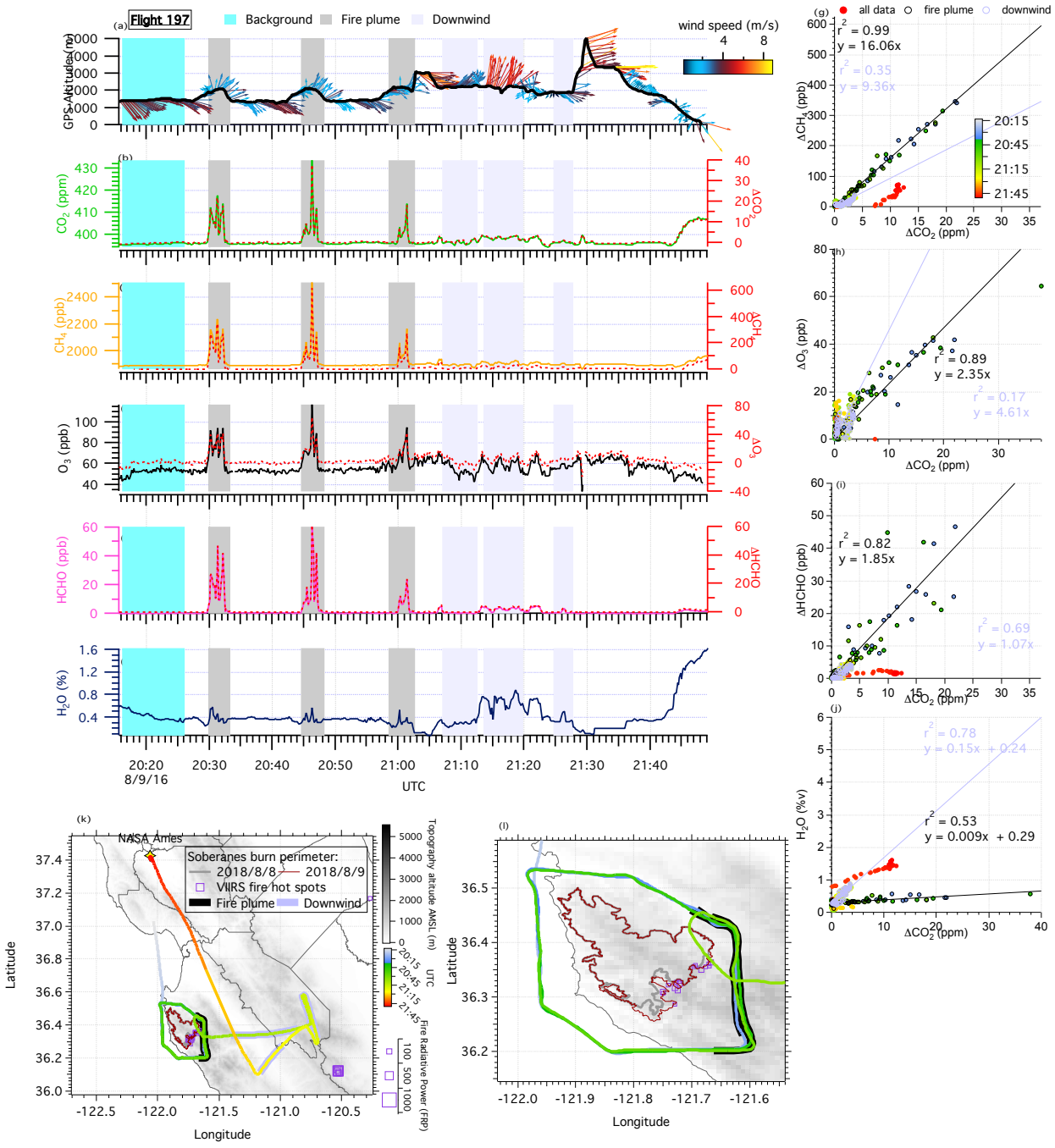

Figure 2. AJAX measurements during the Soberanes fire on August 9, 2016 (Flight 197). The aircraft altitude and wind speed/direction are shown in plot (a) followed by mixing ratios of trace gases in plots (b-f) (left y-axes) and enhanced mixing ratios (right y-axes). The gray bars represent the main fire plume, and the purple bars are aged plume interceptions. Cyan bars indicate the portion of the flight track assigned as background conditions. Scatter plots are shown for enhancements in (g) CH4, (h) O3, (i) HCHO, and (j) H2O vs CO2. The AJAX flight path colored by time and fire burn area for the flight day are shown on topographic maps (k-l), with VIIRS

fire hot spots sized by FRP. Figures for additional AJAX flights are available at doi: 10.5067/ASDC/AJAX/wildfire.

3 Application: Emission Ratio Calculations

The Emission Ratio (ER) of a trace gas, X, is calculated by finding the excess mixing ratio with respect to its average background mixing ratio ($\Delta X = X_{plume} - X_{bkgd}$) and then dividing by the excess mixing ratio of a reference gas (RG), which is usually CO or CO_2 (Andreae & Merlet, 2001), shown in Equation 1. Since the AJAX payload does not include CO, we use enhanced mixing ratios of CO_2 (ΔCO_2) to calculate ERs for various trace gases.

$$ER = \frac{X_{plume} - X_{bkgd}}{RG_{plume} - RG_{bkgd}} = \frac{\Delta X}{\Delta RG} \quad (1)$$

The ERs reported in this work were calculated as the slope between ΔX and ΔCO_2 using an unconstrained linear orthogonal distance regression, forcing the intercept through zero (Akagi et al., 2012; Yates et al., 2016; Yokelson et al., 1999). Background mixing ratios were determined from sections of flights that were upwind of a specific fire, but for Flights 137, 200, and 216, there were not obviously clean periods to select. For these cases, the 10th percentile of seasonal data for a specific trace gas is used as the background. (When tested on other flights, this method resulted in values typically within 1σ standard deviation of the "upwind leg" value.) ER values for individual flight segments are presented in Tables 1-3.

This application is demonstrated for Flight 197, shown in Fig. 2 (g-i). The excess mixing ratios of trace gases were higher in the fresh plume (data points outlined in black) compared to the aged smoke (indicated in purple). The slopes of these lines lead to ERs in the fresh fire plume of: 16.1 ppb CH_4 (ppm CO_2)$^{-1}$, 2.4 ppb O_3 (ppm CO_2)$^{-1}$, and 1.9 ppb HCHO (ppm CO_2)$^{-1}$. In the aged fire plume the ERs are lower: 9.4 ppb CH_4 (ppm CO_2)$^{-1}$ and 1.1 ppb HCHO (ppm CO_2)$^{-1}$, and a strong linear correlation between ΔO_3 and ΔCO_2 was not observed in the aged fire plume.

Ten fires were located in areas that burned primarily evergreen forests, and the other 3 fires (i.e., Mineral, Thomas, and Rocky fire) were located in areas that burned primarily chaparral fuels. ERs ranged 6.1 – 26.8 ppb CH_4 (CO_2)$^{-1}$, 2 – 8.3 ppb O_3 (ppm CO_2)$^{-1}$, and 1.1 – 2.7 ppb HCHO (ppm CO_2)$^{-1}$ from evergreen fires with plume ages ≤8 hr. For chaparral fires, only one ER associated with a plume age ≤ 8 hr was determined (Rocky fire); the methane ER value was consistent with those from evergreen fires, but the ozone ER was noticeably higher. Measurements from the Thomas fire represent aged smoke from a chaparral fire (66 hr), and the ERs are 7.12 ppb CH_4 (ppm CO_2)$^{-1}$ and 0.61 ppb HCHO (ppm CO_2)$^{-1}$ (no O_3 measurements).

ERs were compared across different fires and correlated with meteorological parameters (daily maximum temperature, relative humidity and average wind speed, Fig. 3 (d-f)), 24-hour change in burn area (Fig. 3 (a)), FRP (Fig. 3 (b)) and the average approximated plume age (Fig. 3 (c)) with no significant correlations evident with any variable. Indeed, the variability in emissions and conditions seen on five independent sampling days for a single fire (Soberanes, bar charts insets in Fig. 3) indicates the complexity and dynamic nature of wildfire smoke production and evolution, even within a single event.

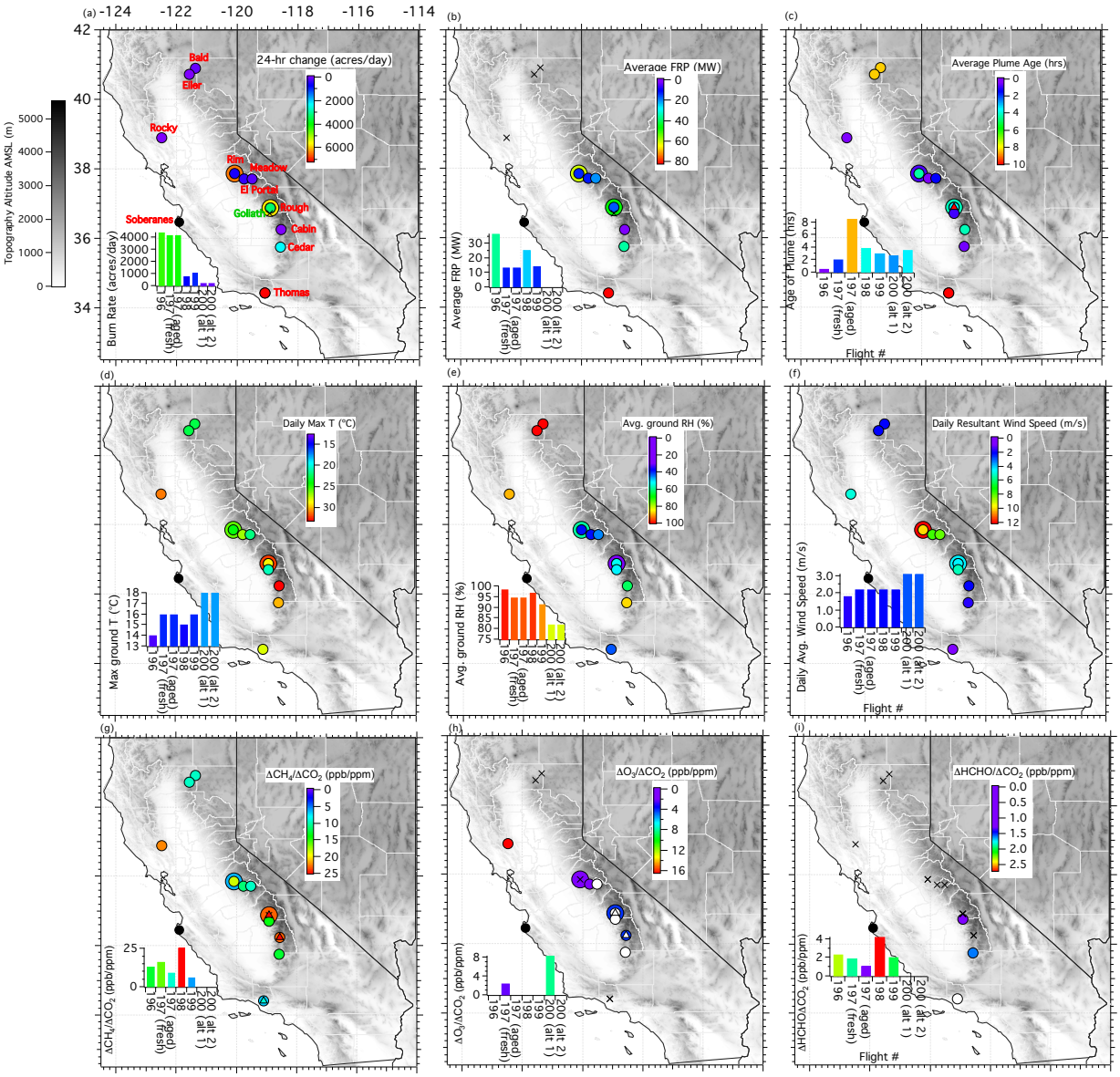

Figure 3. Topographical map showing the wide variety of environmental and fire conditions as well as trace gas observations among the multi-year record. (a) 24-hour change in acres burned; (b) fire radiative power (FRP) averaged for day and time of flight; (c) average plume age; (d) daily maximum temperature, (e) daily average relative humidity, and (f) daily average wind speed at nearby CARB monitoring stations; and (g-i) ERs. Multiple airborne measurements of same fire are shown with multiple circles (outer circle is earlier flight and inner circle is later flight), x markers signify no data, and white circles (ERs only) represent statistically insignificant Pearson's r^2 values between the respective trace gas and ΔCO_2. In plots (c and g-i) fire locations with a circle and a triangle, represent fresh and aged emissions measured within one flight, respectively. Five flights were performed to measure the Soberanes fire, and results are shown in the bar graphs.

The Goliath fire was the only prescribed fire measured between 2013 and 2017, and it was by far the smallest and shortest lived fire in this dataset. The Goliath fire had ERs of 20.7 ppb CH_4 (ppm CO_2)$^{-1}$ and 1.5 ppb HCHO (ppm CO_2)$^{-1}$, with no significant correlation between excess mixing ratios of O_3 and CO_2. These ERs are within the ranges reported for similar evergreen forest wildfires measured in this study.

Table 2. Information on each California fire measured by AJAX in 2015. Units are in square brackets.*Indicates that the fire source location is Rough fire due to more abundant VIIRS hot spots when compared to the Cabin fire.

Fire	**Rocky**	**Cabin**	**Rough**	
Vegetation Types	Chamise chaparral shrubland	Douglas fir Sugar pine Tanoak forest	Douglas fir Sugar pine Tanoak forest	
Total Acres Burned	69,636	6980	151,623	
Duration of Fire	7/29/15–8/14/15	7/19/15–09/05/15	7/31/15–11/5/15	
Flight Date (Flight #)	8/5/15 (166)	8/19/15 (167)		9/2/15 (168)
Avg. RH at Ground Site [%]	89	63	30	54
Max. Temperature at Ground Site [°C]	31	33	32	29
Resultant Wind Speed at Ground Site (m/s)	5.0	2.2	4.5	4.5
Avg. Fire Radiative Power (±1σ) (FRP)	N/A	2.7 (±0)	46.7 (±69.3)	17.5 (±26.0)
Avg. GPS altitude in fire plume (±1σ) [km]	2.7 (±0.6)	2.0 (±0.3) (fresh)	1.1 (±0.6) (aged)	4.5 (±0.7)
Age of fire plume (±1σ) [hr]	0.5	4.3	17.4	3.3
Avg. Distance from Fire Source (±1σ) [km]	23.4 (±6.5)	37.2 (±19.6)*	140.2 (±20.9)*	49.8 (±27.5)
Average H_2O in plume (±1σ) [%v]	0.51 (±0.23)	0.73 (±0.22)	0.89 (±0.24)	0.35 (±0.17)
Max ΔCH_4 in plume [ppb]	118.9	475.4	391.4	-
Max ΔCO_2 in plume [ppm]	7.2	32.8	9.0	-
Max ΔO_3 in plume [ppb]	89.9	148.7	-	-
ER_{CH4}	22.1	22.9	72.1	-
ER_{O3}	16.4	4.3	-	-

276 **Table 3.** Information on each California fire measured by AJAX in 2016 and 2017. Units are in
277 square brackets. "N/A" indicates data which are not available due to instrument failure.
278

Fire	**Goliath** (prescribed)	**Soberanes**						**Cedar**	**Thomas**	
Vegetation Types	Douglas fir Sugar pine Tanoak forest	Redwood Tanoak forest						Jeffrey pine, Ponderosa pine Douglas fir, Black oak	Coastal sage shrubland	
Total Acres Burned	759	103,242						29,322	281,893	
Duration of Fire	6/11/16 – 6/17/16	7/22/16–10/12/16						8/16/16–9/30/16	12/04/17–01/20/18	
Flight Date (Flight #)	6/15/16 (191)	7/28/16 (196)	8/9/16 (197)		8/12/16 (198)	8/24/16 (199)	9/14/16 (200)	8/24/16 (199)	12/13/17 (216)	
Avg. RH at Ground Site [%]	52	96	96		97	94	98	87	43	
Max. Temperature at Ground Site [°C]	21	28	23		22	24	24	30	28	
Resultant Wind Speed at Ground Site (m/s)	5.4	1.8	2.2		2.2	2.2	3.1	1.8	1.0	
Avg. Fire Radiative Power (±1σ) (FRP)	N/A	36.7 (±60.9)	13.4 (±8.0)		25.5 (±19.8)	14.2 (±5.8)	N/A	35.2 (±24.8)	81.8 (±103.8)	
Avg. GPS altitude in fire plume (±1σ) [km]	2.7 (±1.2)	3.0 (±0.02)	2.0 (±0.2) (fresh)	2.1 (±0.1) (aged)	1.4 (±0.1)	3.0 (±0.1)	Alt. 1: 1.3 (±0.4)	Alt. 2: 3.0 (±0.03)	3.8 (±0.3)	0.9 (± 0.1) (ocean)	0.7 (±0.2) (coast)
Age of fire plume (±1σ) [hr]	1.0	0.5	2.0	8.5	3.9	3.0	2.7	3.5	0.6	66.0	
Avg. Distance from Fire Source (±1σ) [km]	12.6 (±9.1)	5.0 (±2.7)	12.9 (±2.3)	70.3 (±18.6)	24.1 (±4.6)	7.6 (±0.6)	26.1 (±7.0)	19.3 (±4.4)	6.1 (±3.0)	441.4 (±66.6)	
Average H_2O in plume (±1σ) [%v]	0.65 (±0.21)	1.00 (±0.07)	0.34 (±0.08)	0.47 (±0.20)	0.93 (±0.06)	0.70 (±0.02)	0.87 (±0.15)	0.12 (±0.03)	0.55 (±0.09)	0.15 (±0.08), 0.43 (±0.15)	
Max ΔCH_4 in plume [ppb]	559.6	1159.1	619.1	38.4	67.4	179.5	-	-	2862.4	56.6	377.0
Max ΔCO_2 in plume [ppm]	38.8	90.5	37.9	3.5	3.9	27.2	-	-	228.1	7.8	36.7
Max ΔO_3 in plume [ppb]	-	-	64.6	-	-	38.5	-	-	-	N/A	N/A
Max ΔHCHO in plume [ppb]	44.9	174.0	60.2	4.3	8.0	49.1	-	-	282.8	8.1	2.2
ER_{CH4}	13.7	13.0	16.1	9.4	25.5	6.1	-	-	12.9	7.1	9.3
ER_{O3}	-	-	2.4	-	-	2.1	-	-	-	N/A	N/A
ER_{HCHO}	1.3	2.3	1.9	1.1	2.7	2.1	-	-	1.6	0.8	0.1

279

4 Conclusion

This new calibrated and quality-controlled data set increases the number of observations of ozone, carbon dioxide, formaldehyde and winds near to a variety of active fires and broadens the range of fire types and conditions for which trace gases and winds were measured. Figure 3 is a visual representation of the variability of meteorological and fire conditions which generated the emissions sampled in situ, as well as the range of ERs obtained in the analysis of emissions from 12 wildfires and 1 prescribed fire in California over a 4+ year period. This work highlights the individuality and variability observed over multiple fires, over multiple years and seasons, and reinforces the difficulty in assigning a single emission factor to a certain fire type or condition.

This data set and the associated preliminary analyses are available to be used in conjunction with satellite data for FRP or trace gas observations, as validation data for smoke plume modeling, or other aggregate studies of the evolution of fire emissions and impacts over decades influenced by climate change. Five flights were made to the Soberanes fire, providing a set of measurements throughout the lifetime of this prolonged incident. Downwind legs and regional transits are also included in the database, making possible contributions to studies of human exposure at regional scales.

Acknowledgments

The NASA AJAX project recognizes support from Ames Research Center Director's funds, the NASA Postdoctoral Program, the NASA OCO-2 Science Team, and the California Air Resources Board (Contract No. 17RD004), as well as by NASA's Atmospheric Composition Program through the Internal Scientist Funding Model. LTI acknowledges support from the NASA Earth Science Research and Analysis Program during data collection and analysis. Technical contributions from T. Tanaka, Z. Young, T. Trias, W. Gore, and E. Quigley made this project possible. The authors gratefully recognize the support and partnership of H211 L.L.C., with particular thanks to K. Ambrose, T. Grundherr, R. Simone, B. Quiambao, J. Lee, and R. Fisher. Data discovery, accessibility and archiving were made possible through the efforts of the Atmospheric Science Data Center staff: K. Phillips, M. Buzanowicz, N. Jester, N. Arora, and S. Haberer.

Open Research

The in situ airborne data described in this manuscript are freely available at NASA's Atmospheric Science Data Center via 10.5067/ASDC/AJAX/wildfire (Iraci et al., 2021). The data are provided in ICARTT format, which is described at https://earthdata.nasa.gov/esdis/eso/standards-and-references/icartt-file-format.

Meteorological data were obtained from the CARB Air Quality and Meteorological Information System (AQMIS) website (https://www.arb.ca.gov/aqmis2/aqmis2.php). Fire Radiative Power (FRP) data were obtained from NASA's Visible Imaging Radiometer Suite (VIIRS) 375 m fire data aboard the National Polar-orbiting Partnership (S-NPP) satellite (https://earthdata.nasa.gov/earth-observation-data/near-real-time/firms). Land cover data were

obtained from the US Geological Survey National Land Cover Database (NLCD) at https://viewer.nationalmap.gov/basic/#startUp. Back trajectories were computed using the Hybrid Single-Particle Lagrangian Integrated Trajectory (HYSPLIT) model (https://www.ready.noaa.gov/HYSPLIT.php). NOAA's Hazard Mapping System (HMS) Fire and Smoke Analysis product was accessed via https://www.airnowtech.org/navigator .

A summary table containing flight-by-flight data is compiled in a comma separated variable file which is freely available at 10.5067/ASDC/AJAX/wildfire. A subset of that information is represented in Tables 1-3 herein.

Note to Editor and Reviewers: The permissions are in process for public access to this data set at doi: 10.5067/ASDC/AJAX/wildfire. If complete public access has not been finalized before review begins, we can arrange an alternative method of access in consultation with Atmospheric Science Data center personnel (POC: kasey.e.phillips@nasa.gov).

References

Aguilera, R., Corringham, T., Gershunov, A., & Benmarhnia, T. (2021). Wildfire smoke impacts respiratory health more than fine particles from other sources: observational evidence from Southern California. *Nature Communications,* 12, 1493. https://doi.org/10.1038/s41467-021-21708-0

Akagi, S. K., Yokelson, R. J., Wiedinmyer, C., Alvarado, M. J., Reid, J. S., Karl, T., Crounse, J. D., & Wennberg, P. O. (2011). Emission factors for open and domestic biomass burning for use in atmospheric models, *Atmospheric Chemistry and Physics*, 11(9), 4039-4072. doi: 10.5194/acp-11-4039-2011

Akagi, S. K., Craven, J. S., Taylor, J. W., McMeeking, G. R., Yokelson, R. J., Burling, I. R., et al. (2012). Evolution of trace gases and particles emitted by a chaparral fire in California, *Atmospheric Chemistry and Physics*, 12(3), 1397-1421. doi: 10.5194/acp-12-1397-2012

Andreae, M. O., & Merlet, P. (2001). Emission of trace gases and aerosols from biomass burning, *Global Biogeochemical Cycles*, 15(4), 955-966. doi: 10.1029/2000GB001382

Buysse, C. E., Kaulfus, A., Nair, U., & Jaffe, D. A. (2019). Relationships between particulate matter, ozone, and nitrogen oxides during urban smoke events in the Western US, *Environmental Science & Technology*, 53, 12519−12528. doi: 10.1021/acs.est.9b05241

CARB (2021) https://ww2.arb.ca.gov/our-work/programs/wildfires, accessed November 2021.

CARB (2019) Air Quality and Meteorological Information System (AQMIS), accessed 2019. https://www.arb.ca.gov/aqmis2/aqmis2.php

Chen, H., Winderlich, J., Gerbig, C., Hoefer, A., Rella, C. W., Crosson, E. R., et al. (2010). High-accuracy continuous airborne measurements of greenhouse gases (CO_2 and CH_4) using the cavity ring-down spectroscopy (CRDS) technique, *Atmospheric Measurement Techniques*, 3(2), 375-386. doi: 10.5194/amt-3-375-2010

Earthdata (2019) NRT VIIRS: 375 m Active Fire Product VNP14IMGT, accessed 2019. https://earthdata.nasa.gov/earth-observation-data/near-real-time/firms

Gao, H. & Jaffe, D. A. (2017) Comparison of ultraviolet absorbance and NO-chemiluminescence for ozone measurement in wildfire plumes at the Mount Bachelor Observatory. *Atmospheric Environment*, 166, 224e233. http://dx.doi.org/10.1016/j.atmosenv.2017.07.007

Gupta, P., Doraiswamy, P., Levy, R., Pikelnaya, O., Maibach, J., Feenstra, B., et al. (2018). Impact of California fires on local and regional air quality: The role of a low-cost sensor network and satellite observations. *Geohealth*, 2(6), 172-181. doi: 10.1029/2018GH000136

Hamill, P., Iraci, L. T., Yates, E. L., Gore, W., Bui, T. P., Tanaka, T., et al. (2016), A new instrumented airborne patform for atmospheric research, *Bulletin of the American Meteorological Society*, 97(3), 397-404. doi: 10.1175/bams-d-14-00241.1

Hersbach, H., Bell, B., Berrisford, P., Hirahara, S., Horányi, A., Muñoz-Sabater, J., et al. (2020). The ERA5 global reanalysis, *Quarterly Journal of the Royal Meteorological Society*, 146, 1999-2049. doi:10.1002/qj.3803

Holden, Z. A., Swanson, A., Luce, C. H., Jolly, W. M., Maneta, M., Oyler, J. W., et al., (2018). Decreasing fire season precipitation increased recent western US forest wildfire activity. *Proceedings of the National Academy of Sciences*, 115, E8349-E8357.

Iraci, L. T., Yates, E. L., Marrero, J. E., Parworth, C. L., Ryoo, J.-M., Tanaka, T. (2021) Compendium of Airborne Trace Gas Measurements Collected in and around California Fire Plumes by the AJAX Project, Atmospheric Science Data Center, initial release, doi: 10.5067/ASDC/AJAX/wildfire

Jaffe, D. A., O'Neill, S. M., Larkin, N. K., Holder, A. L., Peterson, D. L., Halofsky, J. E., et al. (2020) Wildfire and prescribed burning impacts on air quality in the United States, *Journal of the Air & Waste Management Association*, 70(6), 583-615. doi: 10.1080/10962247.2020.1749731

Liu, Y., Kochanski, A., Baker, K. R., Mell, W., Linn, R., Paugam, R., et al. (2019). Fire behaviour and smoke modelling: Model improvement and measurement needs for next-generation smoke research and forecasting systems. *International Journal of Wildland Fire*, 28, 570–588. https://doi.org/10.1071/WF18204

Long, R. W., Whitehill, A. Habel, A., Urbanski, S., Halliday, H., Colón, M., et al. (2021). Comparison of ozone measurement methods in biomass burning smoke: an evaluation under field and laboratory conditions, *Atmospheric Measurement Techniques*, 14, 1783–1800. https://doi.org/10.5194/amt-14-1783-2021

McClure, C. D., & Jaffe, D. A. (2018), US particulate matter air quality improves except in wildfire-prone areas. *Proceedings of the National Academy of Sciences*, 115(31), 7901–7906. doi: 10.1073/pnas.1804353115

Ottmar, R. D., Sandberg, D. V. , Riccardi, C. L. , & Prichard, S. J. (2007). An overview of the Fuel Characteristic Classification System — Quantifying, classifying, and creating fuelbeds for resource planning. *Canadian Journal of Forest Research*, 37(12), 2383-2393. doi: 10.1139/X07-077

Radeloff, V. C., Helmers, D. P., Kramer, H. A., Mockrin, M. H., Alexandre, P. M., Bar-Massada, A., et al. (2018). Rapid growth of the US wildland-urban interface raises wildfire risk. *Proceedings of the National Academy of Sciences,* 115, 3314-3319. https://doi.org/10.1073/pnas.1718850115

Riccardi, C. L., Ottmar, R. D., Sandberg, D. V., Andreu, A., Elman, E., Kopper, K., et al. (2007). The fuelbed: A key element of the Fuel Characteristic Classification System. *Canadian Journal of Forest Research*, 37(12), 2394-2412. doi: 10.1139/X07-143.

Singh, H. B., Anderson, B. E., Brune, W. H., Cai, C., Cohen, R.C., Crawford, J.H., et al. (2010). Pollution influences on atmospheric composition and chemistry at high northern latitudes: Boreal and California forest fire emissions. *Atmospheric Environment*, 44(36), 4553-4564. doi: https://doi.org/10.1016/j.atmosenv.2010.08.026

St. Clair, J. M., Swanson, A. K., Bailey, S. A., Wolfe, G. M., Marrero, J. E., **Iraci**, L. T., et al. (2017). A new non-resonant laser-induced fluorescence instrument for the airborne in situ measurement of formaldehyde, *Atmospheric Measurement Techniques,* 10, 4833-4844. doi:10.5194/amt-10-4833-2017

Stein, A. F., Draxler, R. R, Rolph, G. D., Stunder, B. J. B., Cohen, M. D., & Ngan, F., (2015). NOAA's HYSPLIT atmospheric transport and dispersion modeling system. *Bulletin of the American Meteorological Society*, 96, 2059-2077. http://dx.doi.org/10.1175/BAMS-D-14-00110.1

Tadic, J. M., Loewenstein, M., Frankenberg, C., Butz, A., Roby, M., Iraci, L.T., et al. (2014). A comparison of in situ aircraft measurements of carbon dioxide and methane to GOSAT data measured over Railroad Valley playa, Nevada, USA. *IEEE Transactions on Geoscience and Remote Sensing*, 52, 7764-7774. doi: 10.1109/TGRS.2014.2318201

Tanaka, T., Yates, E. L., Iraci, L. T., Johnson, M. S., Gore, W., Tadic, J. M., et al. (2016). Two-year comparison of airborne measurements of CO_2 and CH_4 with GOSAT at Railroad Valley, Nevada, *IEEE Transactions on Geoscience and Remote Sensing*, 54, 4367-4375. doi:10.1109/TGRS.2016.2539973

Walters, S. P., Schneider, N. J., & Guthrie, J. D. (2011). Geospatial Multi-Agency Coordination (GeoMAC) wildland fire perimeters, 2008, Report Rep. 612, Reston, VA.

Westerling, A. L., Hidalgo, H. G., Cayan, D. R., & Swetnam, T. W. (2006). Warming and earlier spring increase Western U.S. forest wildfire activity, *Science*, 313(5789), 940.

Yates, E. L., Iraci, L. T., Roby, M. C., Pierce, R. B., Johnson, M. S., Reddy, P. J., et al. (2013). Airborne observations and modeling of springtime stratosphere-to-troposphere transport over California, *Atmospheric Chemistry and Physics*, 13(24), 12481-12494. doi: 10.5194/acp-13-12481-2013

Yates, E. L., Iraci, L. T., Singh, H., Tanaka, T., Roby, M. C., Hamill, P., et al. (2016), Airborne measurements and emission estimates of greenhouse gases and other trace constituents from the 2013 California Yosemite Rim wildfire, *Atmospheric Environment,* 127, 293-302. doi: https://doi.org/10.1016/j.atmosenv.2015.12.038

Yokelson, R. J., Goode, J. G., Ward, D. E., Susott, R. A., Babbitt, R. E., Wade, D. D., et al. (1999). Emissions of formaldehyde, acetic acid, methanol, and other trace gases from biomass fires in North Carolina measured by airborne Fourier transform infrared spectroscopy. *Journal of Geophysical Research*, 104(D23), 30109-30125. doi: 10.1029/1999JD900817